Journal of Nematology 35(3):244–251. 2003.

Fine Structure of the Stoma of *Bunonema* sp. and *Teratorhabditis palmarum* (Nematoda) and Its Phylogenetic Significance

C. M. Dolinski and J. G. Baldwin[1]

Abstract: Fine structure of the stoma, including the cheilostom, gymnostom, and stegostom of *Bunonema* sp. and *Teratorhabditis palmarum* was compared with *Caenorhabditis elegans* to consider fine structural characters that may be phylogenetically informative. The stegostom, enclosed by the anterior end of the pharynx, includes a triradiate lumen surrounded by radial cells (interradial or pairs of adradial cells) repeated in the dorsal and subventral sectors; in Rhabditina, typically the stegostom includes anteriorly two sets of epithelial and posteriorly two sets of muscular radial cells. These muscle cells are anteriorly m1 and posteriorly m2. In *Bunonema* sp., unlike *T. palmarum* and *C. elegans,* the stegostom has a third set of interradial epithelial cells. In *Bunonema* sp., m1 is expressed by three interradial cells, whereas in *T. palmarum* and *C. elegans* m1 is three pairs of adradial muscle cells (i.e., six cells). In all three taxa m2 is expressed as three pairs of adradial muscle cells. Posterior processes of adjacent adradial cells fuse, and closely apposed nuclei may present a figure-eight shape. However, in *Bunonema* the three interradial m1 cells each have a long posterior process enclosing two separate round nuclei. In combination with additional characters, these diverse stoma features may prove phylogenetically informative. Specifically, the radial epithelial cells of the stegostom appear to be a synapomorphy consistent with a bunonemid-diplogastrid-rhabditid clade, whereas a thickening in the dorsal sector of the stoma cuticle lining is interpreted as a synapomorphy supporting a bunonemid-diplogastrid clade.

Key words: *Bunonema* sp., *Caenorhabditis elegans,* cell fusion, DAPI, Diplogastrina, fine structure, nuclei, SEM, TEM, *Teratorhabditis palmarum.*

The position of *Bunonema* Jägerskiöld, 1905 and *Teratorhabditis* (Osche, 1952) Dougherty, 1953 was not resolved with other Rhabditina Chitwood, 1933 (sensu Andrássy, 1984) in an 18s rRNA-based phylogeny (Blaxter et al., 1998) and, indeed, the unusual morphology, particularly of *Bunonema,* further underscores the need for careful consideration of evolutionary relationships. *Bunonema,* together with other Bunonematoidea Micoletzky, 1922, is unique in its asymmetry; its body wall cuticle has complex lace-like ornamentation on the right side and deep longitudinal ridges on the left side. Nevertheless, these nematodes generally are considered rhabditids because they appear with light microscopy to have a rhabditid-like cylindrical stoma and three-part pharynx. Although Andrássy (1984) places *Bunonema* within Rhabditina, Sudhaus (1976) and Sudhaus and Fitch (2001), in their phylogeny of Rhabditidae Örley, 1880, do not include *Bunonema,* apparently considering this and similar genera as part of the outgroup.

Fine structure of the stoma has been demonstrated to include phylogenetically useful characters that could be applied to further test phylogenetic relationships of *Bunonema* and *Teratorhabditis* to other Secernentea. The basic stoma pattern for Rhabditina is believed to include four sets of radial cells in the stegostom where the anterior two sets, e1 and e3, are interradial epithelia, followed posteriorly by two sets of muscle cells, respectively named m1 and m2 (Albertson and Thomson, 1976; Baldwin et al., 1997a; Wright and Thomson, 1981). In some taxa, m1 and (or) m2 are expressed by interradial muscle cells, whereas in others a pair of adradial muscle cells occurs in the position otherwise occupied by an interradial muscle cell (De Ley et al., 1995). It has been predicted that *Teratorhabditis* shares the basic stoma pattern with other Rhabditina.

The stoma is distinctive in other Secernentea. In Diplogastrina and Rhabditina (sensu Andrássy, 1984) the stoma pattern apparently has anterior sets of interradial epithelia (Baldwin et al., 1997b), whereas analogous epithelial cells are absent in Cephalobina Andrássy, 1974 (De Ley et al., 1995; Dolinski et al., 1998; van de Velde et al., 1994). The stoma of *Bunonema,* however, has been especially difficult to interpret by light microscopy due to the nematode's asymmetry and small size, as well as the elaborate and, therefore, relatively opaque cuticle. Recently, however, Fürst von Lieven (2002) hypothesized apomorphies, including features of the stoma observed by light microscopy, to suggest bunonemids as sister taxa to diplogastrids. Of particular interest is a longitudinal fold of thinner cuticular material describing as occurring in the gymnostom and connecting with a dorsal bulge of the stegostom in both *Bunonema* spp. and Diplogastrina (Fürst von Lieven, 2002). Transmission electron microscopy (TEM) of the stoma could provide additional character data relevant to resolving phylogenetic relationships.

Materials and Methods

Nematode cultures and maintenance: Bunonema sp., strain JB 116, isolated from a garden compost at the residence of J. G. Baldwin is an undescribed new spe-

Received for publication 23 January 2003.

[1] Department of Nematology, University of California, Riverside, California 92521. Current address of C. Dolinski is Universidade Estadual do Norte Fluminense, CCTA/LPP, Av. Alberto Lamego, 2000 Parque Califórnia, Campos dos Goytacazes, RJ, Brazil, 28013-600.

The authors thank David Fitch for nematode strains as well as Ricardo Souza and Paul De Ley for critical reading of the manuscript. We especially thank M. Mundo-Ocampo for contributing SEM of *Bunonema.* This work was supported by Brazilian Conselho Nacional de Desenvolvimento Científico e Tecnológico (CNPq), Brazil, to C. Dolinski; U.S. National Science Foundation Grants DEB-9318249 to J. G. Baldwin and W. K. Thomas; DEB 97-12355 to S. A. Nadler and J. G. Baldwin; and DEB-0228692 to W. K. Thomas, J. G. Baldwin, P. De Ley, D. H. Fitch, and S. A. Nadler.

E-mail: claudia.dolinski@censa.com.br; james.baldwin@ucr.edu

This paper was edited by R. T. Robbins.

cies. *Teratorhabditis palmarum,* strain DF 5019, was extracted from the cocoons of *Rhynchophorus palmarum* (palm weevil) in Trinidad and Tobago by R. Giblin-Davis. Both strains were grown on nematode growth media (NGM) with *Escherichia coli* as the food source at 25 °C (Brenner, 1974; Sulston and Hodgkin, 1988).

Scanning electron microscopy (SEM): For SEM, nematodes were fixed in 5% aqueous formaldehyde, rinsed in several changes of 0.1 M phosphate buffer (pH 7.0), postfixed overnight in 4.0% aqueous osmium tetroxide solution, and again rinsed in several changes of cold 0.1 M phosphate buffer. Dehydration was through a series (20–100%) of absolute ethanol, and critical point drying was in a Tousimis Autosamdri-810 critical point dryer. Specimens were mounted on double-sticking copper tape attached to aluminum stubs. Stubs with mounted nematodes were coated for 3 minutes with a 25-nm layer of gold palladium in a Hummer V sputter coater, and specimens were observed with an XL30-FEG Phillips 35 scanning electron microscope at 10 kV.

Transmission electron microscopy (TEM): For TEM, adult females of *Bunonema* sp. and *T. palmarum* were kept alive on ice until embedding in 3% agar at 38 °C. After the agar hardened, a block enclosing each nematode was cut out, removed, and then fixed in 2% osmium tetroxide solution in 0.1 M sodium cacodylate buffer (pH 7.2) for 2 hours with constant agitation at room temperature. They were rinsed seven times (10 minutes each) with 1% sodium chloride (NaCl), pre-stained overnight with 1% aqueous uranyl acetate at room temperature, rinsed again seven times with 1% NaCl, dehydrated with serial acetone solutions (20–100%), and infiltrated with epoxy resin (Spurr, 1969). Serial sections with silver refraction (75 nm) were obtained using a Sorvall MT-6000 ultramicrotome, and the sections were mounted on 50 mesh-copper grids coated with 0.9% pioloform. Sections from three specimens of each species were post-stained with lead citrate (Reynolds, 1963) and observed on a Hitachi H-600 TEM at 75 kV.

Visualization of nuclei: Nuclei of particular cells were visualized with a combination of TEM and 4′,6-diamidino-2-phenylindole (DAPI) fluorescent microscopy using methods previously described by Dolinski et al. (1998). Ten females each of *T. palmarum* and *Bunonema* sp. were fixed, mounted on slides, and stained with DAPI solution as described by Dolinski et al. (1998). Slides were sealed with Vaseline and observed on a Zeiss microscope fitted with UV source and filters to excite the DAPI/DNA complex at 360 nm (Whittaker et al., 1991).

Results

Bunonema: The stoma of *Bunonema* sp. is enclosed by a complex asymmetric framework specialized from the outermost layers of the body wall cuticle. The anterior end of the stoma is enclosed within an offset head with dorsal and ventral elongate bifid cuticular extensions (Figs. 1A; 2). The right side of the head includes a single amphid opening; SEM and TEM indicate the amphid is absent on the left lateral side (Fig. 2B). The stoma opening is about 3 to 4 μm posterior to the tip of the extensions (Figs. 1A; 2). In longitudinal view the cuticular walls of the lumen are underlined anteriorly by hypodermis (lining the cheilostom) followed posteriorly by arcade syncytia, a1 and a2 (lining the gymnostom), and posteriorly by radial and marginal cells of the anterior end of the pharynx (lining the stegostom) (Fig. 1A,B).

The cheilostom is short and asymmetrical, forming an oblique cylinder, offset to the left lateral side (Fig. 1A). The predominant gymnostom is highly flexible, bending by as much as 90 degrees in both living and fixed individuals. Throughout most of its length the gymnostom is delimited by a slightly concave dorsal and two subventral cuticular plates, and near the junction with the stegostom the dorsal plate is thickened (Fig. 3A–D).

The stegostom is less than one-fourth the length of the gymnostom and although its flexibility is relatively limited, in many specimens the junction with the gymnostom is oblique with the dorsal side relatively anterior. The stegostom lumen is nearly triradiate, but asymmetry is further established throughout the stegostom by relative thickening of the dorsal cuticular plate; the dorsal gland duct penetrates this plate (Fig. 3D,E). The cuticular lining of the stegostom is surrounded by a pattern of radial cells repeated in the dorsal and two subventral sectors and separated by a marginal cell at each apex (Figs. 1B; 3H,I). Each single marginal cell extends the entire length of the stegostom. The radial cells from the anterior end are designated e1, e3, e4, m1, and m2 (Figs. 1A,B; 3F–I); e1, e3, and e4 are epithelial cells, and m1 and m2 are muscle cells. Whereas e1, e3, and e4 and m1 each consist of one interradial cell per triradiate sector, m2 each include one pair of adradial cells per triradiate sector (i.e., six adradial cells) (Figs. 1B; 3H,I), each with a long process extending posterior to the stegostom. As viewed in transverse section, interradial m1 cells anteriorly are each partly divided, suggesting a V-shape (Figs. 1B; 2H), and the posterior process of each cell has two separate round nuclei (Figs. 1C; 5A). Anteriorly, each pair of adradial m2 cells is separated by m1 cells, neurons, and posterior processes of e1, e3, and e4 (Fig. 3I). Posterior to the stegostom, adradial pairs of m2 fuse and nuclei of the pair form a figure-eight shape (Fig. 5A).

Teratorhabditis palmarum: Although the lip region is less elaborate than in *Bunonema* sp. and the stoma opening is not offset, the stoma of *T. palmarum* includes a cheilostom and elongate gymnostom that otherwise are similar in position and general structure to those of *Bunonema* (Fig. 1D). The cuticle lining of the gymnostom of *T. palmarum* is continuous and nearly uniform in

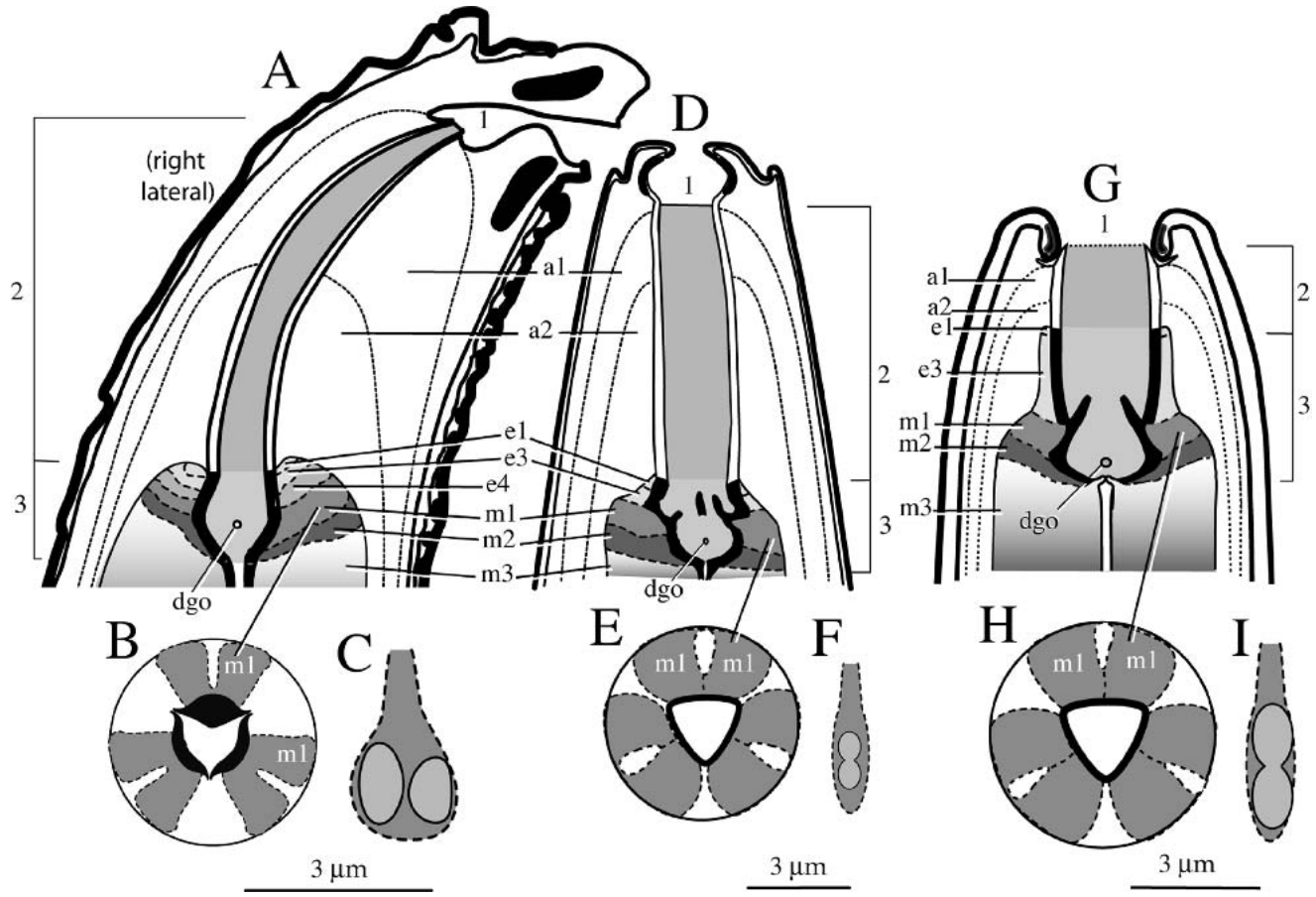

FIG. 1. Comparative diagrams of the stomas reconstructed from serial transmission electron micrographs. (A–C) *Bunonema* sp. A) Longitudinal view through the subventral sectors. B) Transverse view including the deeply infolded m1 interradial muscle cells. C) Longitudinal representation of an m1 muscle cell round nuclei. (D–F) *Teratorhabditis palmarum.* D) Longitudinal view through subventral sectors. E) Transverse view including the m1 adradial muscle cells. F) Longitudinal representation of the posterior process of an adjacent pair of adradial m1 muscle cells showing a figure-eight-shaped nucleus pair. (G–I) *Caenorhabditis elegans.* G) Longitudinal view through subventral sectors. H) Transverse view including the adradial m1 muscle cells (Albertson and Thomson, 1976; De Ley et al., 1995). I) Longitudinal representation of the posterior process of an adjacent pair of adradial m1 muscle cells showing a figure-eight-shaped nucleus pair (a1, a2, respective arcade syncytia; dgo dorsal gland orifice; e1, e3, e4, respectively, epithelial cells; m1, m2, m3, respectively, muscle cells; 1, cheilostom; 2, gymnostom; 3, stegostom. Illustrations of *C. elegans* redrawn from Baldwin et al. (1997b) and Dolinski et al. (1998).

thickness, without a dorsal thickening (Fig. 4A,B). The stegostom includes an arrangement of marginal and radial cells similar to that of *Bunonema* but differing by the absence of e4 epithelial interradial cells (Figs. 1D,E; 4C–F). The anterior portion of the stegostom is lined by cuticle not distinguishable from that of the gymnostom and enclosed by e1 and e3 interradial cells (Fig. 4C,D). The thinner cuticle lining associated with m1 includes three flexible protrusions (so-called "teeth") that extend into the lumen (Figs. 1D; 4D,E). Further posteriorly, the cuticle lining of the stegostom consists of a dorsal and two subventral concave plates, and each plate is associated with a pair of adradial m2 muscles. The anterior end of the m2 adradial pair flanks a portion of the m1 adradial cells as well as neurons and posterior processes of interradial epithelial cells (Fig. 4F). Unlike *Bunonema,* in *T. palmarum* each pair of adjacent adradial m1 cells fuse posteriorly and adjacent nuclei of the pair form a figure-eight shape; in this respect, posteriorly m2 cells of *T. palmarum* are similar to m1 cells (Figs. 1E,F; 5A,B; Table 1).

Unlike *C. elegans, Bunonema* and *T. palmarum* are particularly opaque and nuclei are somewhat obscured by denser tissue. In addition, stoma nuclei are relatively smaller in *T. palmarum* and occur in multiple focal planes. Nevertheless, careful observation of DAPI fluorescence combined with TEM was suitable to confirm nuclei numbers and shape.

DISCUSSION

Transmission electron microscopy of the stoma of *Bunonema* sp. and *T. palmarum* reveals new features that may prove useful for testing phylogenetic hypotheses when compared to other Rhabditina including *Caenorhabditis elegans* and Diplogastrina (Albertson and Thomson, 1976; Baldwin et al., 1997a, 1997b; De Ley et al., 1995; Endo and Nickle, 1994, 1995; Fürst von

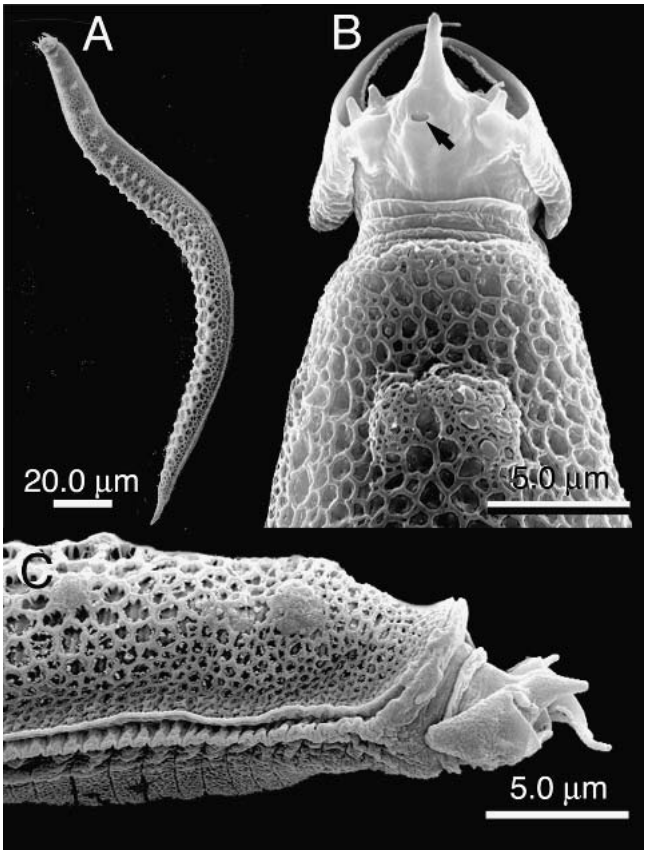

FIG. 2. Scanning electron micrograph of female of *Bunonema* sp. A) Entire individual. B) Right lateral view of anterior end. Arrow indicates amphid opening. C) Ventral view of anterior end.

Lieven, 2002; Wright and Thomson, 1981). Whereas the cheilostom and gymnostom are conserved, varying among species primarily in length and orientation, the stegostom appears to be rich in phylogenetically informative characters and character states. The dorsal "longitudinal fold of thinner cuticle" in the gymnostom previously described by light microscopy for *Bunonema* (Fürst von Lieven, 2002) was not specifically confirmed by TEM. However, posteriorly the dorsal lining of the gymnostom is slightly thickened and this thickening is increasingly predominant posteriorly in the stegostom where the thickening is penetrated by the dorsal gland orifice. This stegostom thickening may indeed by a synapomorphy with similar thickening expressed in diplogastrids, and might be homologous, in some diplogastrids, with a dorsal tooth through which the gland orifice opens (Baldwin et al., 1997b).

In the stegostom, the numbers of sets of interradial epithelial cells vary within Rhabditina ranging from one set (e.g., *Heterorhabditis bacteriophora* and perhaps *Pelodera* sp.), or two sets (e1 and e3) in *T. palmarum* and most other Rhabditina (e.g., *C. elegans*) and Diplogastrina (e.g., *Aduncospiculum halicti*), to a unique three-set arrangement, including e4 in *Bunonema* sp. (Baldwin et al., 1997a, 1997b; De Ley et al., 1995; Endo and Nickle, 1994, 1995). Notably, the epithelial cells of *Bunonema* and *T. palmarum,* unlike *C. elegans,* are not configured to form a narrow pharyngeal collar, although we note that anteriorly the stegostom is narrowly tapered in *T. palmarum* (Figs. 1D; 4A,D). Secernentea other than Rhabditina and Diplogastrina, including Cephalobidae (Cephalobina), lack interradial epithelial cells in the stegostom; in Cephalobidae, cells developmentally homologous to e1 and e3 are not part of the adult pharynx and instead become hypodermal cells or are programmed to die (Dolinski et al., 1998). Thus, the presence of radial epithelial cells at the anterior end of the stegostom appears to be a synapomorphy defining the rhabditid-diplogastrid clade, and the presence of these cells is consistent with placement of *Bunonema* within such a clade. However, the presence of e4 may be an autapomorphy for the Bunonematoidea.

The stegostoms of *Bunonema* sp. and *T. palmarum* each include two sets of interradial muscle cells as other Rhabditina (Baldwin et al., 1997a, 1997b; De Ley et al., 1995; Wright and Thomson, 1981). However, *Bunonema* sp. differs from some other Rhabditina by m1 that consists of three interradial cells whereas m2 is comprised of three pairs of cells giving six adradial muscle cells. In *T. palmarum* and*C. elegans,* m1 and m2 each consist of six adradial muscle cells (Albertson and Thomson, 1976; De Ley et al., 1995; Dolinski et al., 1998; Wright and Thomson, 1981) (Fig. 1H). The same arrangement of cells also occurs in *Pelodera* sp. and *H. bacteriophora* (De Ley et al., 1995; Endo and Nickle, 1994).

Observations of nuclei associated with m1 and m2 cells suggest an intermediate state in which the cells proper remain separate, but posterior processes of certain adjacent cells merge. In some cases figure-eight-shaped nuclei, visible with TEM and DAPI stain, suggest two nuclei closely apposed or partly fusing (Figs. 1F,I; 5;

FIG. 3. Transmission electron micrographs of *Bunonema* sp. A) Transverse section through anteriormost end of gymnostom (g). B) Transverse section through gymnostom (g) about 5 µm posterior to Fig. 3A. C) Transverse section near posterior end of gymnostom (g) including dorsal thickening (asterisk) of the cuticle lining. D) Longitudinal section including junction (arrows) of gymnostom and stegostom. Lining of the lumen (l) including dorsal thickened (asterisk) penetrated by the dorsal gland duct (dgd) (a, arcade syncytium). E) Near transverse section through the stegostom (s) showing the dorsal thickening (asterisk) of the cuticle lining near the region of the dorsal gland duct (dgd). m2 adradial muscles flank the dorsal gland region. Due to asymmetry, the ventral side of the section extends anterior to the stegostom. F) Longitudinal section through subventral sector showing three sets of interradial epithelial cells (e1, e3, e4) and a portion of adradial muscle cells m1 and m2 (s, stegostom). G) Longitudinal section through adradial muscle cells m1 and m2 (s, stegostom). H) Transverse section through adradial muscle cells m1 adjacent to the stegostom (s) (mc, marginal cell). I) Transverse section through adradial m2 cells. Anteriorly the two cells flank a region adjacent to the stegostom (s) that includes m1 muscle cells as well as nerve and posterior processes of e1, e2, and e3 epithelial cells (mc, marginal cell). Broken line indicates m2 cell membranes.

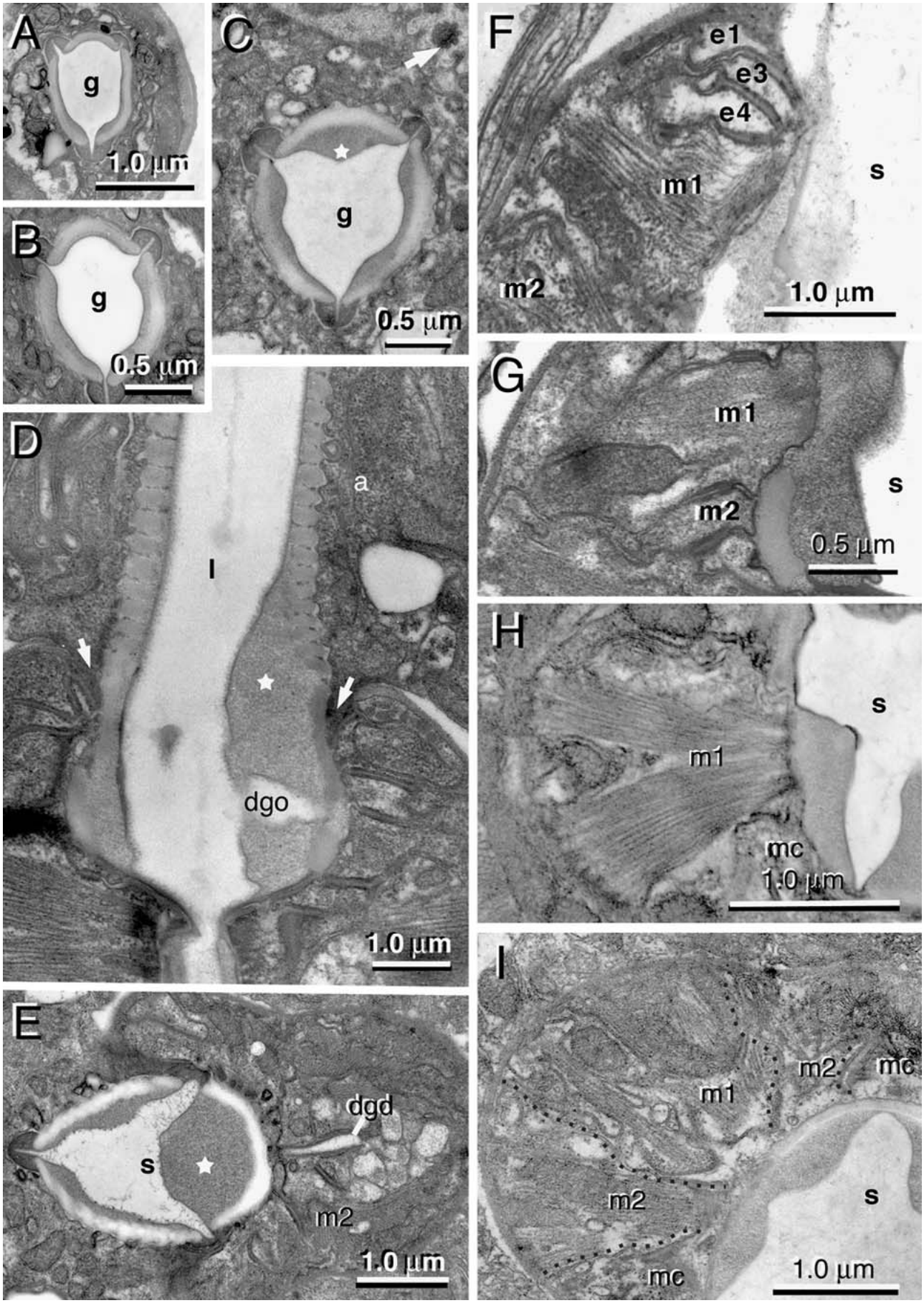
A
g
1.0 µm
B
g
0.5 µm
C
g
0.5 µm
D
a
l
dgo
1.0 µm
E
dgd
s
m2
1.0 µm
F
e1
e3
e4
m1
s
m2
1.0 µm
G
m1
s
m2
0.5 µm
H
s
m1
mc
1.0 µm
I
m2
mc
m1
m2
s
mc
1.0 µm

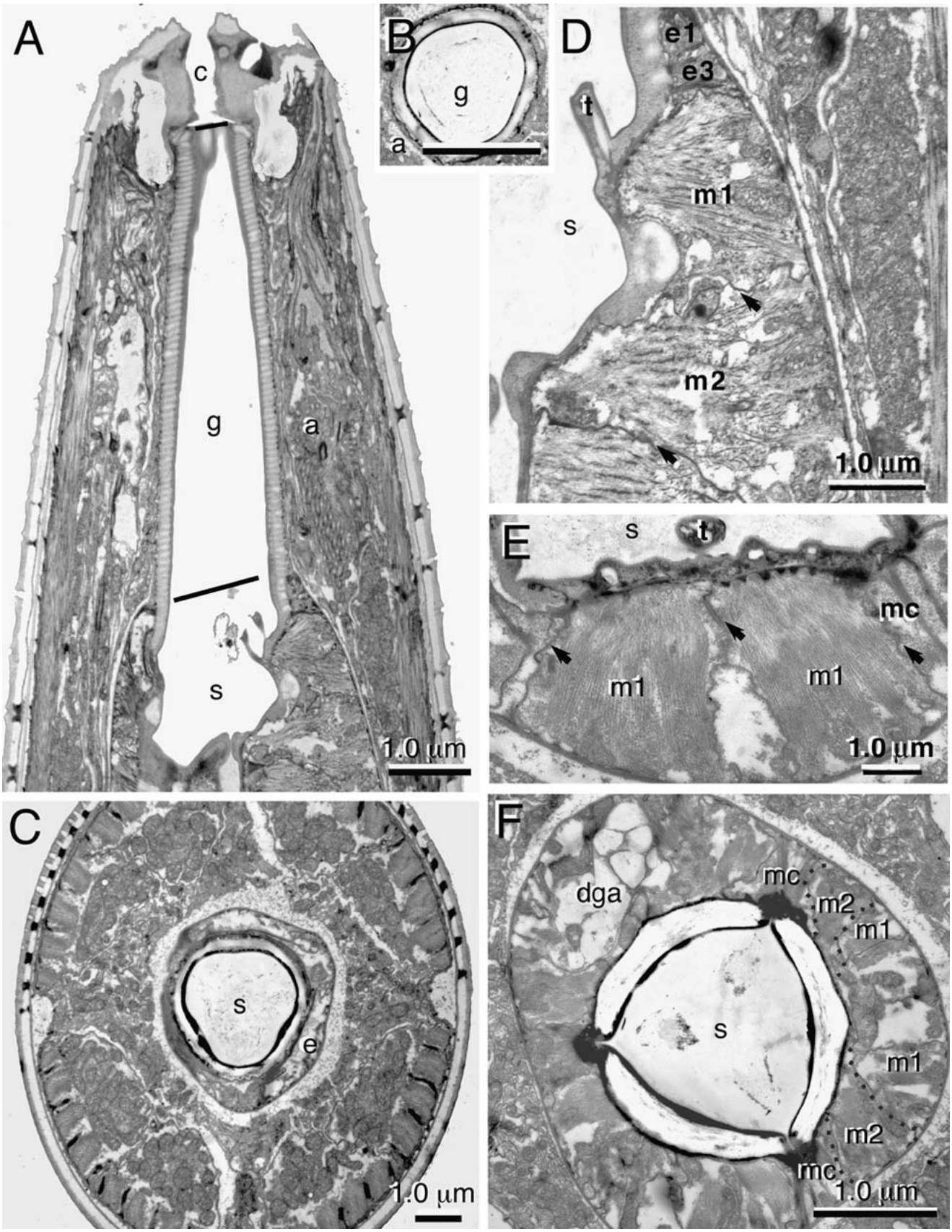

FIG. 4. Transmission electron micrographs of *Teratorhabditis palmarum*. A) Longitudinal section through the stoma including cheilostom (c), gymnostom (g), and stegostom (s). B) Transverse section through gymnostom (g) surrounded by arcade syncytia (a). Scale bar is 1 µm. C) Transverse section through the anterior end of the stegostom (s) including interradial epithelial cells (e). D) Longitudinal section through subventral sector showing two sets of interradial epithelial cells (e1, e3) and adradial muscle cells m1 and m2. Arrows indicate boundaries between cells (s, stegostom; t, "tooth"). E) Transverse section through adradial muscle cells m1 and adjacent marginal cells (mc) surrounding the stegostom (s) (t, "tooth"). Arrows indicate boundaries between cells. F) Transverse section through adradial muscle cells m2 flanking a region that includes m1 muscles (dga, dorsal gland ampulla; mc, marginal cell). Broken line indicates m2 cell membranes.

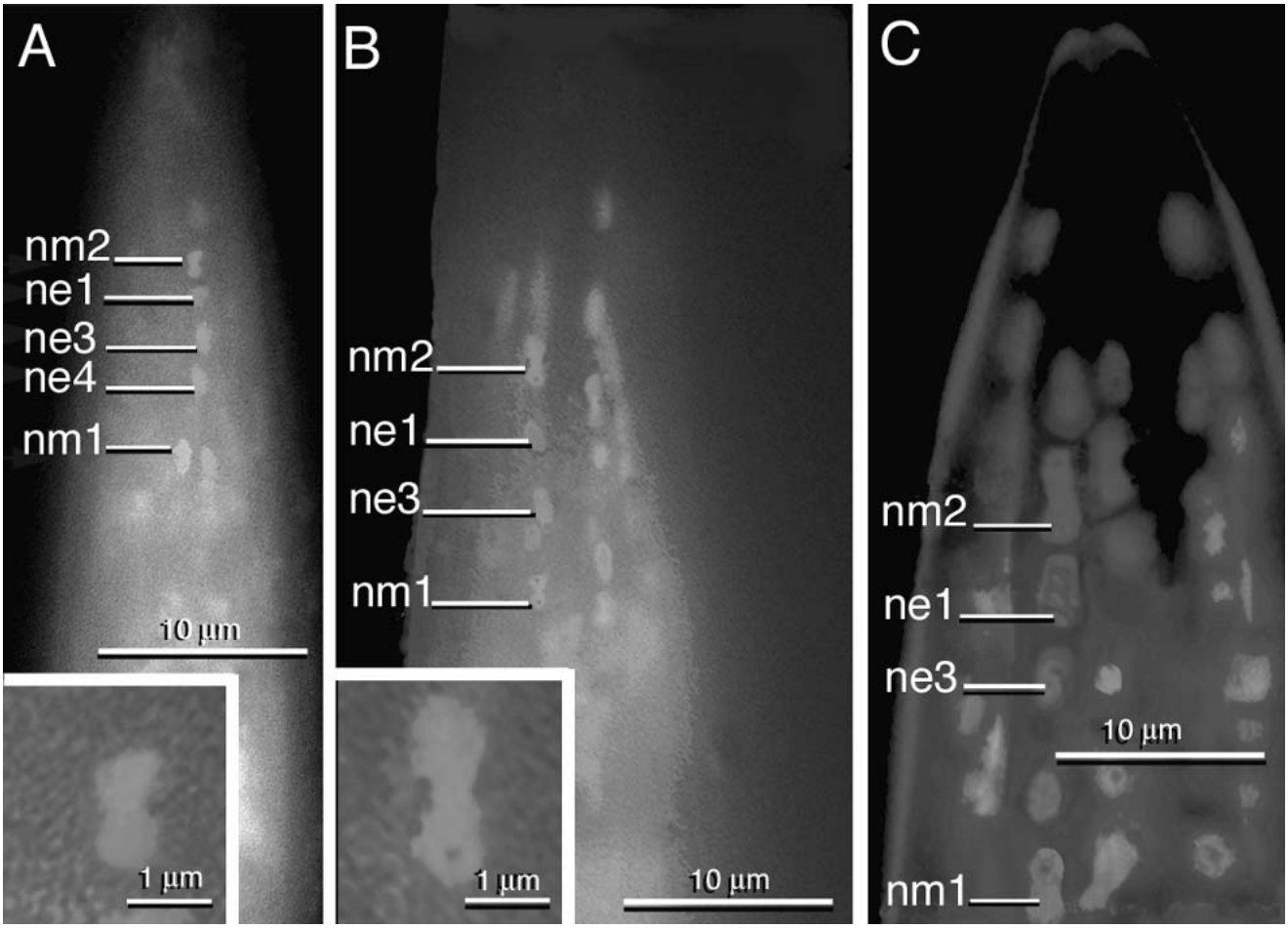

FIG. 5. DAPI-stained nuclei in the anterior end showing nuclei from cells associated with stoma. Cell/nucleus association is based on prior TEM. A) *Bunonema* sp. showing figure-eight-shaped nuclei (nm2) in adradial muscle cell m2. Note round interradial epithelial (ne1, ne3, ne4) and m1 nuclei (nm1). Inset is enlargement of figure-eight-shaped nm2. B) *Teratorhabditis palmarum* showing figure-eight-shaped nuclei in both adradial muscle cells m1 (nm1) and m2 (nm2). Inset is enlargement of figure-eight-shaped nm2. Note round interradial epithelial (ne1, ne3). C) *Caenorhabditis elegans* showing the same arrangement as in *T. palmarum.* Adapted from Fig. 3A of Dolinski et al. (1998).

Table 1). In this respect m1 cells vary among the taxa examined. In *Bunonema* the three interradial m1 cells each have two separate single round nuclei. In *T. palmarum* and *C. elegans* adjacent adradial pairs of m1 as well as m2 cells each have fused posterior processes, and the merging nuclei are figure-eight-shaped (Figs. 1C,F,I; 5). One interpretation is that in *Bunonema* sp. the three interradial m1 cells are the result of fusion of adradial cells in which their two round nuclei remain separate. The posterior processes of pairs of the six adradial cells of m2 in *Bunonema* as well as m1 and m2 in *T. palmarum* all fuse posteriorly and have paired figure-eight-shaped nuclei (Figs. 1C,F; 5A,B).

Fine structure of the stoma suggests that *Bunonema* sp. and *T. palmarum* share derived characters with other rhabditids, but within this framework there also are variable character states with respect to numbers of epithelial radial cells as well as numbers and apparent degrees of fusion of pairs of muscular radial cells and their nuclei. They further support the previous hypothesis of stegostom radial epithelial cells as a synapomorphy defining the rhabditid-diplogastrid clade (Baldwin

TABLE 1. Differential ultrastructural characters of the stegostom.

	Bunonema sp.	*T. palmarum*	*C. elegans*
dorsal relative to subventral plates	thickened	not thickened	not thickened
e-4 interradial cells	present	absent	absent
m1, number of radial cells	3 interradial	6 adradial	6 adradial*
m1, number and shape of nuclei	6/round	6 (3 pair)/figure-8-shaped	6 (3 pair)/figure-8-shaped

* Previously in *C. elegans,* m1 was described as syncytial ring and m2 as three cells (Albertson and Thomson, 1976) but De Ley et al. (1995) described both m1 and m2 as three adradial pairs.

et al., 1997a, 1997b) and the longitudinal modification of the dorsal wall of the stoma as a possible synapomorphy of a bunonemid-diplogastrid clade (Fürst von Lieven, 2002). In combination with additional morphological and molecular characters, these features of the stoma may prove to be particularly useful in a phylogenetic analysis and may help to address difficulties in resolving these relationships with 18S rRNA data alone.

Literature Cited

Albertson, D. G., and J. N. Thomson. 1976. The pharynx of *Caenorhabditis elegans*. Philosophical Transactions of the Royal Society of London Series B 275:299–325.

Andrássy, I. 1984. Klasse Nematoda (Ordnungen Monhysterida, Desmocolecida, Araeolaimida, Chromadorida, Rhabditida). Stuttgart, Germany: Gustav Fischer Verlag.

Baldwin, J. G., L. M. Frisse, J. T. Vida, C. D. Eddleman, and W. K. Thomas. 1997a. An evolutionary framework for the study of developmental evolution in a set of nematodes related to *Caenorhabditis elegans*. Molecular Phylogenetics and Evolution 8:249–259.

Baldwin, J. G., R. M. Giblin-Davis, C. D. Eddleman, D. S. Williams, J. T. Vida, and W. K. Thomas. 1997b. The buccal capsule of *Aduncospiculum halicti* (Nemata: Diplogasterina): An ultrastructural and molecular phylogenetic study. Canadian Journal of Zoology 75:407–423.

Blaxter, M. L., P. De Ley, J. R. Garey, X. L. Liu, P. Scheldeman, A. Vierstraete, J. R. Vanfleteren, L. Y. Mackey, M. Dorris, L. M. Frisse, J. T. Vida, and W. K. Thomas. 1998. A molecular evolutionary framework for the phylum Nematoda. Nature 392:71–74.

Brenner, S. 1974. The genetics of *Caenorhabditis elegans*. Genetics 77:71–94.

De Ley, P., M. C. Van De Velde, D. Mounport, P. Baujard, and A. Coomans. 1995. Ultrastructure of the stoma in Cephalobidae, Panagrolaimidae, and Rhabditidae with proposal for a revised stoma terminology in Rhabditida (Nematoda). Nematologica 41:153–182.

Dolinski, C., G. Borgonie, R. Schnabel, and J. G. Baldwin. 1998. Buccal capsule development as a consideration for phylogenetic analysis of Rhabditida (Nemata). Developmental Genes and Evolution 208:495–503.

Endo, B. Y., and W. R. Nickle. 1994. Ultrastructure of the buccal cavity region and oesophagus of the insect parasitic nematode, *Heterorhabditis bacteriophora*. Nematologica 40:379–398.

Endo, B. Y., and W. R. Nickle. 1995. Ultrastructure of anterior and mid-regions of infective juveniles of *Steinernema feltidae*. Fundamental and Applied Nematology 18:271–294.

Fürst von Lieven, A., 2002. The sister group of the Diplogastrina (Nematoda). Russian Journal of Nematology 10:127–137.

Reynolds, E. S. 1963. The use of lead citrate at high pH as an electron-opaque stain in electron microscopy. Journal of Cell Biology 17:208–222.

Spurr, A. R. 1969. A low-viscosity epoxy resin embedding medium for electron microscopy. Journal of Ultrastructural Research 26:31–43.

Sudhaus, W. 1976. Vergleichende Untersuchungen zur Phylogenie, Systematik, Ökologie, Biologie und Ethologie der Rhabditidae (Nematoda). Zoologica 125:1–229.

Sudhaus, W., and D. Fitch. 2001. Comparative studies on the phylogeny and systematics of the Rhabditidae (Nematoda). Journal of Nematology 33:1–70.

Sulston, J. E., and J. Hodgkin. 1988. Methods. Pp. 587–606 *in* W. B. Wood, ed. The nematode *Caenorhabditis elegans*. Plainview, New York: Cold Spring Harbor Laboratory Press.

van de Velde, M. C., P. De Ley, D. Mounport, P. Baujard, and A. Coomans. 1994. Ultrastructure of the buccal cavity and the cuticle of three Cephalobidae (Nematoda: Rhabditida). Nematologica 40:541–563.

Whittaker, S. L., R. C. Shattock, and D. S. Shaw. 1991. Variation in DNA contents of nuclei of *Phytophthora infestans* as measured by a microfluorometric method using the fluorochrome DAPI. Mycological Research 95:602–610.

Wright, K. A., and J. N. Thomson. 1981. The stoma of *Caenorhabditis elegans* (Nematoda: Rhabditoidea): An ultrastructural study. Canadian Journal of Zoology 59:1952–1961.